Tanzania Journal of Science 47(1): 214-227, 2021
ISSN 0856-1761, e-ISSN 2507-7961

Capacity Analysis of a Television White Space Network Deployed under Distance Distribution Approach

Moses Ismail*, Mussa Kissaka and Prosper Mafole
Department of Electronics and Telecommunications Engineering, College of Information and Communication Technologies, University of Dar es Salaam,
P. O. Box 33335, Dar es Salaam, Tanzania
Corresponding author, e-mail: moses82004@gmail.com
Co-authors' e-mails: mkissaka@yahoo.com; mafole@gmail.com
Received 17 Sep 2020, Revised 12 Dec 2020, Accepted 28 Dec 2020, Feb 2021
https://dx.doi.org/10.4314/tjs.v47i1.19

Abstract

Television White Space (TVWS) is currently a leading technology for broadband connectivity in rural areas due to its penetration capability and robustness to attenuation and fading. Since most rural areas where TVWS is suitable are characterized by sparse population distribution, a deployed network must be adequately planned to provide the required coverage while meeting the targeted quality of service. This paper modelled and analyzed the capacity of a TVWS suitable for sparsely populated settings. The TVWS network was modelled using the distance distribution approach, and capacity simulation was carried out through Matlab. Results showed that, at the signal quality of just 10 dB, a network of one BS and 10 CPEs (Customer Premise Equipment), achieved a channel capacity of 18 Mbps and user downlink capacity of 2 Mbps. These results are better than the trials conducted in a similar environment in the sub-Saharan Africa region.

Keywords: TVWS, CPE, SINR, Rural Broadband, PPP.

Introduction

Although wireless networks have become imperative in our daily lives, exponential growth in the number of user devices and applications put a massive demand on rapidly congesting spectrum (Struzak et al. 2015). As a result, large parts of the communities lack broadband connectivity as network service providers prioritize this scarce and expensive resource (World Bank 2018). In most developing countries, the problem is dire, with the Internet penetration of just 35% of the global average (Miniwatts 2020). Traditionally, cellular wireless networks deliver broadband services to remote areas; however, low returns on investment (RoI) have made it expensive to deploy such networks in sparsely populated areas. The emergence of the Television White Space (TVWS) provides an opportunity to curb this growing spectrum shortage. Studies show that most developing countries possess a hugely untapped TVWS spectrum (Ismail et al. 2019). One of the studies conducted in Nigeria showed a TVWS percentage availability of up to 80% in some areas (Abu and Ufoaroh 2019). In South Africa, a study by Lysko et al. (2014) showed the availability of up to 90% in rural areas. In Tanzania, the availability of TVWS is more than 80% in most regions. For instance, a study conducted in Dodoma region has shown the availability of the TVWS to be close to 100% for 80% of the time (Matogoro et al. 2018). Coincidentally, the TVWS' penetration and bandwidth benefits make it possible to offload broadband networks at a relatively low-costs, especially in areas where traditional approaches cannot realize the returns on investment.

In the last decade, rapid developments in TVWS have been witnessed, including standardization and testing via several trials across the world. The wireless standards in TVWS specified by the Institute of Electrical and Electronics Engineers (IEEE) include IEEE 802.11af for Wireless Local Area Network (WLAN), IEEE 802.15.4m for Wireless Personal Area Network (WPAN), IEEE 802.22 for Wireless Regional Area Network (WRAN), IEEE 802.19.1 for coexistence and the European Computer Manufacturers Association (ECMA)'s ECMA-392 which is a medium access control (MAC) and physical (PHY) layers standard for operation in TVWS. Both 802.11af and IEEE 802.22 are focused on providing long-range connectivity in rural areas with IEEE 802.22 covering a range up to 30 km (IEEE 2011, IEEE 2012). While IEEE 802.11af supports time division multiple access (TDMA), IEEE 802.22 supports orthogonal frequency division multiple access (OFDMA), making it a suitable candidate for long-range broadband communication (Sum et al. 2013). The white space WLAN parallels the popularly used wireless fidelity (Wi-Fi) and has come to be known as White-Fi. While Wi-Fi has been successful in offloading broadband networks, it is still too prone to interference as it operates in ISM bands. This leads to it achieving short-range coverage with many nodes required to cover users spread over wider areas. Since it operates in a much lower band, white-fi can achieve higher range and capacity as it is less prone to interference and fading, making it economically viable for low-income and sparsely populated areas (Johnson et al. 2016). The white-fi architecture includes a white space geolocation database (WSGDB) that protects the primary (television) network by appropriately allocating the network resources like power and channels. White space devices (WSDs) report their locations to the WSDBs every time they change locations based on a set distance threshold. Depending on the type of the WSD, the WSDBs return the permissible power and the available channels over which the transmission should take place. Various regulators including, Office of Communications (Ofcom) in the UK, Federal Communications Commission (FCC) in the USA, European Conference of Postal and Telecommunications Administrations (CEPT) in Europe and others, have developed frameworks for secondary usage of the TVWS (Nyasulu et al. 2018, Stirling and Beveridge 2019). An overview of WSDs and regulations are presented in the study by Amine and Aawatif (2017).

Unlike most cellular networks deployment, which is planned for specific areas, the white-fi, like Wi-Fi, networks are randomly deployed for particular target users, depending on needs. To take advantage of the penetration benefits of TVWS, the location, spacing and radial coverage of the network nodes need to be specifically optimized to provide the highest capacity possible. Most studies and trials used power allocation schemes to characterize the secondary user capacity. Such studies include the ones by Hessar and Roy (2015), Kalliovaara et al. (2018) and Dore et al. (2018). To utilize the penetration benefits of TVWS and reach many sparsely populated users at good SINR, a conceptual model of a last-mile TVWS network and its capacity analysis based on the distance between the secondary CPEs has been used in this study as proposed by Amine and Aawatif (2017). One area where white-fi is useful is in offloading broadband networks such as LTE and optical fibre, and this has been used as a case in this study. The recent rollout of the National ICT Broadband Backbone (NICTBB) in Tanzania provides a robust and affordable backhaul that reaches up to districts level (Pazi and Chatwin 2013). White-fi clusters can extend the coverage to remote villages in rural areas similar to the model proposed by Kumar et al. (2016). However, unlike the proposal by Kumar et al. (2016) and in the mobile cellular networks, the TVWS penetration is exploited in this case to establish an optimal separation between nodes which is suitable to cover more users and realize optimal capacity in a sparse population setting. This study modelled and analyzed the capacity of a TVWS suitable for sparsely populated settings.

Methodology

This study used the Poisson Point Process (PPP) distribution model for the Customer Premise Equipment (CPEs) in a channel environment characterized by the Hata propagation model. Several studies have shown that the Hata propagation model and its derivatives adequately characterize the pathloss of sub-urban and rural areas (Akinbolati and Ajewole 2020, Dionisio et al. 2015, Fanan et al. 2017, Gao et al. 2020). To exploit the penetration power of TVWS, the optimal separation distance between co-channel CPEs that can ensure reducing interference and optimizing link capacity is established. To simplify the analysis, in this study, all the CPEs have the same configuration, in terms of power, antenna height and gain. This means, at the same distance and environmental condition, the interference power at a target node is the same. Co-channel interference at a target CPE from other CPEs in the same cluster is considered. Due to the high availability of white space channels in the developing world, the channels occupied by TV services have been avoided to simplify the analysis. Using Matlab, the link capacity performance of such a network with CPEs deployed following Poisson distribution of density λ was analyzed. Secondly, attention was turned to a specific CPE and analyzed the capacity of a user connected in that CPE. The parameters used for analysis included co-channel separation, SINR, number of available channels, CPE operational radius and number of nodes covering the target area. The parameter values were obtained from the operating specifications and guidelines from the literature. Since there is no TVWS guideline in Tanzania, a hybrid of FCC and Ofcom from which most other guidelines have been derived was used.

Secondary network capacity

The model consisted of one remote white space base station (WSBS) serving a cluster of customer premise equipment (CPEs). Depending on the size of the remote area that needs to be covered, the number of WSBSs may differ. Figure 1 shows a typical extension of a fibre-based broadband network, where at the point of presence (PoP), the WSBS is connected to the fibre network via a switch powered over Ethernet. A Point to Point (PtP) backhauling strategy is used whereby a link to a specific CPE is within a 30 km range supported by 802.22 (IEEE 2011). A typical service, in this case, could be a streaming service to a school or hospital.

Further applications of TVWS discussed in several previously conducted studies include IoT, telemedicine, smart-farming, smart-grid and others (Hassan et al. 2017, Ismail et al. 2019, Masonta et al. 2015a, b). Depending on the distance from the fibre network, the signal may traverse several WS relays before reaching the final WSBS that serves the intended remote CPEs. In this context, every WSBS and its respective cluster of CPEs is termed as a cell. The CPEs, which are intelligent WS devices, process the TVWS signal to match the 802.11 family of protocols in Wi-Fi access points and user equipment. The WS incompatible end-user devices connect to the last mile network through the Wi-Fi router.

Channel link capacity

Geolocation databases provide a possibility for secondary networks to be arbitrarily deployed as ad-hoc networks—in the similar fashion Wi-Fi deployment is done in 2.4/5 GHz band by ensuring the primary network is protected from the secondary interference (Hessar and Roy 2015). Figure 2 shows a secondary network of multiple CPEs randomly distributed in a specific area co-existing with a primary network. As stated earlier, the CPEs distribution follows a Poisson Point Process (PPP) with density λ. The PPP model represents random location characteristic of base stations which exists in heterogeneous networks when a large number of small cell base stations are deployed. This scenario reflects the user centric-deployment nature of

TVWS, where arbitrary deployment is likely to happen (Yu and Kim 2013).

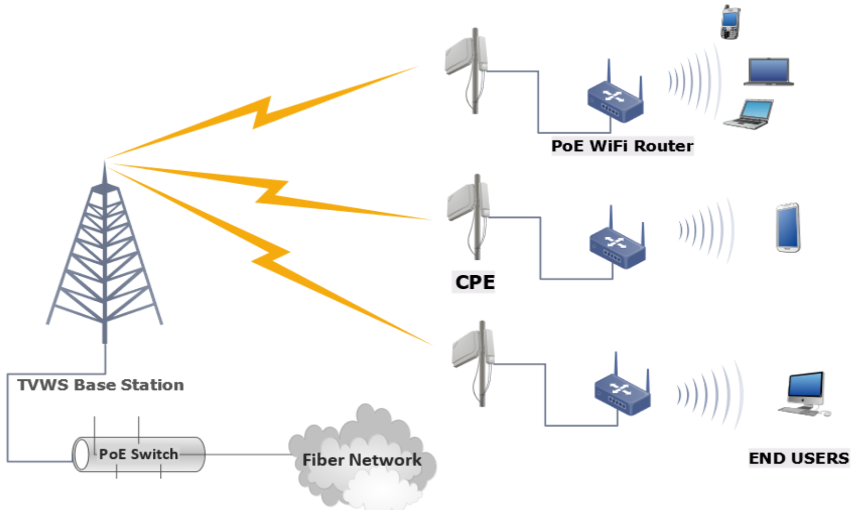

Figure 1: A conceptual model for fiber link extension by TVWS.

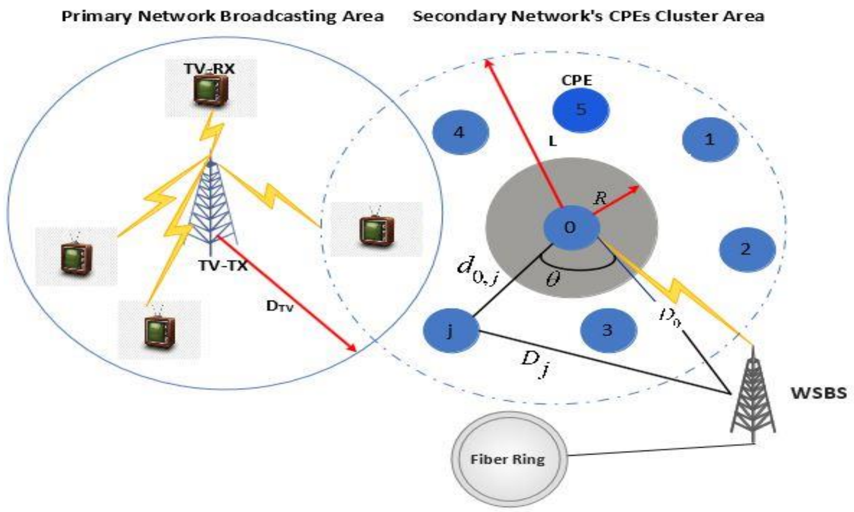

Figure 2: Primary-secondary systems coexistence model.

For a channel of bandwidth B_0, the Shannon capacity for a target CPE (CPE$_0$) in the center of the cluster, C_0 is given as,

$$C_0 = B_0 \log_2(1 + SINR_0) \qquad (1)$$

where $SINR_0$ is the ratio of the received signal power (P_R), at CPE$_0$ to the total interference (I_{CPE_0}) and noise (N_0), given as:

$$SINR_0 = \frac{P_R}{N_0 + I_{CPE_0}} \quad (2)$$

Let $P_{0,j}$, $L_{0,j}$ respectively be the interference power level of the jth CPE and the channel path loss between CPE_0 and the jth CPE situated at a distance $d_{0,j}$ as shown in Figure 2. The total interference at the centre of CPE_0 is;

$$I_{CPE_0} = \sum_{j=1}^{N} I_{CPE_j} + \tau_0 = \sum_{j=1}^{N} \frac{P_{0,j} \left| g_{0,j} \right|^2}{L_{0,j}} + \tau_0 \quad (3)$$

where τ_0 is the self-interference effect in CPE_0, N is the number of interfering CPEs in the cluster and $g_{0,j}$ is a gain between the CPEs. It is assumed that the configuration for all the CPEs is the same, meaning that $P_{0,j} = P_0$ is the same for all CPEs and the channel gain to be symmetric, which means $g_{0,j} = g_{j,0} = g_0$ for all CPEs. Additionally, $\tau_0 \ll \sum_{j=1}^{N} I_{CPE_j}$ thus ignored.

Since the received signal at the CPE_0 from the WSBS undergoes the environmental degradation, it can be expressed as;

$$P_R = \frac{P_w g_w g_0}{L(D_0)} \quad (4)$$

where P_w and g_w are respectively the power and channel gain of the WSBS and $L(D_0)$ is the path loss between the WSBS and CPE_0, which depends on the distance between WSBS and the target CPE, D_0 .

Combining Equations (2), (3) and (4), the SNR_0 can be expressed as,

$$SINR_0 = \frac{P_w g_w g_0}{L(D_0)\left[N_0 + \sum_{j=1}^{N} \frac{P_0 \left| g_0 \right|^2}{L(d_{0,j})} \right]} \quad (5)$$

For the white space network to be beneficial for sparsely populated rural areas, a wider coverage is required, while maintaining good SINR. Therefore, owing to the abundant availability of TVWS, the distance distribution approach was adopted as opposed to power optimization. Uniformly poison point process (PPP) was used as presented by Haenggi (2005) where the distance distribution between a point and its nth neighbour in a two-dimensional plane is given as,

$$f_n(r) = \frac{e^{(-\lambda\pi r^2)^n}}{r\Gamma(n)}; \forall n \in N \quad (6)$$

where; λ denotes the number of nodes per unit surface area and $\Gamma(.)$ is the incomplete gamma function. On the other hand, to achieve the required communication quality, a particular target SINR, γ_T has to be met. The probability that the signal quality will drop below this target value is expressed as,

$$P_{out} = \mathrm{P}_r (SNR_0 \le \gamma_T) \quad (7)$$

Assuming $N_0 \ll \sum_{j=1}^{N} \frac{P_0|g_0|^2}{L(d_{0,j})}$ and using Equation (5), γ_T can be expressed as,

$$\gamma_T = \frac{P_w g_w g_0}{L(D_0)\left[\sum_{j=1}^{N} \frac{P_0 \left| g_0 \right|^2}{L(d_{0,j})} \right]} \quad (8)$$

Assuming equidistant interfering nodes, the distance $d_{0,j}$ between the target CPE (CPE_0) and the jth CPE is deduced from Equation (8) as,

$$d_{0,j} = D = L^{-1}\left(\frac{N\gamma_T L(D_0) P_0 g_0}{P_w g_w}\right) \quad (9)$$

From the CDF of Equation (6), the outage probability of a link to the n-nearest neighbours within a cluster can be extracted as,

$$P_{out} \simeq 1 - e^{(-\lambda\pi D^2)} \sum_{k=1}^{n-1} \frac{(\lambda\pi D^2)^k}{k!} \quad (10)$$

Using Equation (1), and considering P available channels at a target area, the total capacity of the target CPE_0 is expressed as,

$$C_0 \simeq \sum_{k=1}^{P}(1-P_{out})B_k\log_2(1+\gamma_T) \qquad (11)$$

Substituting Equation (10) into Equation (11), the link capacity can be expressed as: -

$$C_0 \simeq \sum_{k=1}^{P}\sum_{q=1}^{N-1} B_k\log_2(1+\gamma_T)\frac{(\lambda\pi D^2)^q}{q!}e^{(-\lambda\pi D^2)} \qquad (12)$$

Cell and user capacity

In this section, cell and average user capacity have been analyzed considering the number of sectors, channel aggregation and the number of nodes per cell. Figure 3 shows a conceptual model where the 802.11n Wi-Fi nodes deliver last-mile service to users. Unlike other Wi-Fi standards, the 802.11n can theoretically offload up to 65-600 Mbps amount of data and is backward compatible with 802.11a, b, and g standards (Karthipan et al. 2016). In addition, it supports MIMO, hence improves the signal in case the last mile coverage extension is required, a scenario more likely to happen under a sparse population setting. Figure 3 depicts such a scenario, where under the extended service set (ESS), one Access Point (AP) extends coverage through other APs (AP2 and AP3). The frame aggregation feature also reduces overhead which ensures that 802.11n maintains the data rate in adapting 802.22 frames; as a result, it is possible to offload the middle mile network at the same data-rate per user in the last mile. As shown in Figure 3, assuming APs pairs operate on different bands and a high-speed Ethernet or fibre cable linking them, the user throughput only depends on the user distance from the access point. In this context, the user refers to an individual accessing the last mile network via the Wi-Fi APs.

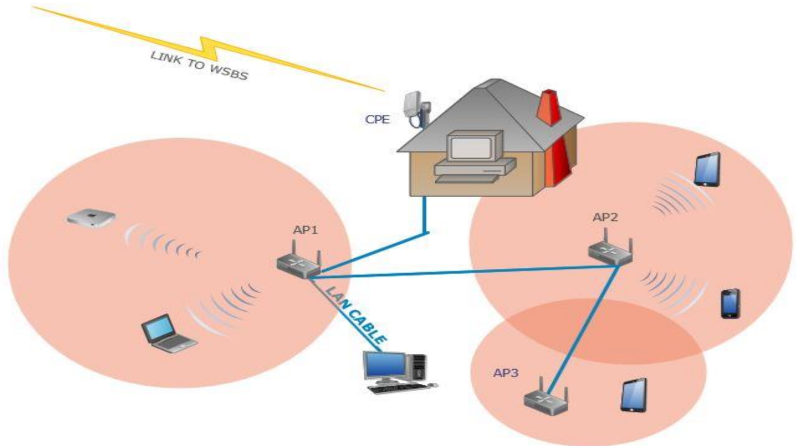

Figure 3: Network access architecture in the last mile.

In this study, a base station providing an omnidirectional coverage in a target area via three white space radio antennas spaced 120° apart was considered. Each radio providing a 120° coverage is referred to as a sector, and three sectors constitute to a cell—an entire geographic region covered by the base station. Depending on the number of channels at a target area, each sector is assigned a specific channel. However, in a case of channels shortage, the self-co-existence allows for IEEE 802.22 superframe to be shared among the cells (Karthipan et al. 2016). For a cell with N_s sectors, the cell capacity, C_p is a total of individual sector capacity C_i given as,

$$C_p = \sum_{i=1}^{N_s} C_i \qquad (13)$$

Assuming equal average capacity per sector with a channel of bandwidth B_s , the capacity per CPE is estimated from Equation (12) as,

$$C_N \simeq \frac{1}{N_S}\sum_{1}^{N_S} \sum_{q=1}^{N} B_s \log_2(1 + \gamma_T) \frac{(\lambda\pi D^2)^q}{q!} e^{(-\lambda\pi D^2)} \quad (14)$$

For a CPE, the capacity for each user depends on the CPE channel capacity and the number of users requesting the service. Since individual users are connected via the Wi-Fi APs with a bandwidth higher than that of the white space CPEs, the CPEs capacity is the limiting factor on the total throughput the end-user can achieve. In this study, the impact of the interference between the Wi-Fi APs to the end-user throughput is not considered. Depending on the distance the user is from the AP, their capacity may vary due to variation in the received signal quality. Typically, not all users will be active in all nodes all the time. Assuming an $\psi:1$ oversubscription, the number of users per cell is given as,

$$N_u = \frac{\psi C_p}{C_N} \quad (15)$$

Because of the large number of channels available in the rural areas, channel aggregation can be implemented to improve the capacity per user at the last mile. In most cases, up to 3 channels of 8 MHz can be aggregated to obtain the channel bandwidth of up to 24 MHz.

Results and Discussion

The study aimed to analyze the capacity of the TVWS network under different network parameters for sparsely populated settings. In Tanzania, the broadband cellular networks are mostly present in urban areas. In contrast, the fibre network has a point of presence at every district, in locations within 10-30 km of rural areas, most of which have no broadband connectivity. This study, therefore, provides a suitable approach to extend coverage to remote locations which are sparsely populated. The analysis was based on the FCC guidelines, which has been adopted by most developing countries, albeit, with some few adjustments in the spectrum range, power and bandwidth (Nyasulu et al. 2018). Most trials conducted in developing countries were within the FCC framework. The differences between existing rules are found in the study by Oh et al. (2014), and the comparison between FCC's and Ofcom's is outlined by Nyasulu et al. (2018). Table 1 shows the parameters adopted for this study. The study considered $\lambda = 0.1$ which translates to a single CPE for a 10 km^2 area (a radius of 1.8 km).

Table 1: Simulation parameters

Parameter	Value
Channel bandwidth	8 MHz
CPE HAAT	10 m
WSBS HAAT	50 m
Gain of the WSBS	11 dB
CPE EIRP	30 dBm
WSBS EIRP	36 dBm
Noise figure	-174 dBm
CPEs density	0.1

In the following section, the channel capacity performance against various network parameters is firstly presented, followed by the numerical evaluation of the user capacity. The network parameters explored in the study include the CPE separation, number of CPEs per WSBS, distance of the CPE from the WSBS, WSBS Effective Isotropic Radiated Power (EIRP) and the CPE's EIRP.

Channel and cell capacity

As stated earlier, the channel capacity depends on the signal quality, i.e. Signal to Noise and Interference Ratio (SNIR), the number of CPEs (N), the WSBS distance from the target CPE (R) and the CPEs separation (D). Figure 4(a) shows the relationship between the SINR and D for a fixed WSBS range. As expected, there is a monotonic increase in SINR with the CPE separation due to reduced interference. Figure 4(b) shows a monotonic decrease of the SINR with WSBS distance from the target CPE, due to weak received power levels as R increases. As Figure 4 depicts, for a given CPEs separation distance, doubling R results in almost 2-folds decay in SINR while doubling D results in nearly double the SINR for a given R.

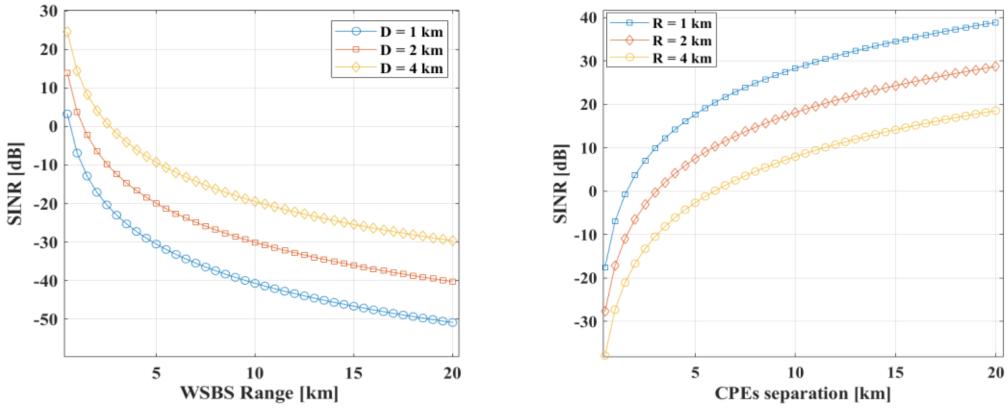

(a) (b)

Figure 4: The variation of SINR with the CPE separation (D) (a) and WSBS range (R) (b) for N = 10.

For the system to be able to deliver the required level of service quality, the target SINR has to be met. Figure 5 shows the channel capacity performance against the CPEs separation for WSBS range of 5 km. As expected from Equation (9), the target SINR increase with increasing D.

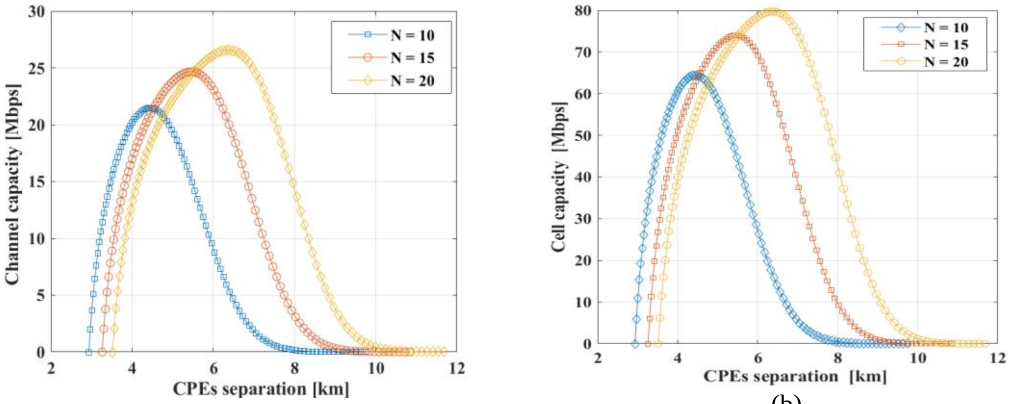

(a) (b)

Figure 5: Capacity vs CPE separation for $SINR_t$ = 10 dB and D_o = 5 km.

Since D depends on the number of CPEs, which in turn affect the SINR; to maintain the required service quality, the separation between CPEs has to increase as N increases. As shown in Figure 5 (a), increasing N while holding D results to channel capacity drop due to interference. Additionally, to achieve a higher capacity for a target SINR, one would need to increase D to maintain interference at the required level for the required signal quality. For instance, to achieve a channel capacity of 22 Mbps at the $SINR_t$ of 10 dB, the CPEs separation is around 4.3 km. However, increasing D by about 1 km, the capacity of 25 Mbps can be achieved with N = 15. For larger D, increasing N should result in higher capacity since interference decreases. However, as shown in Equation (12), the capacity will eventually decrease as D go past a threshold value beyond which a tolerable SINR cannot be achieved. Figure 5 (b) shows the result for a cell with three sectors $N_S = 3$) containing the same number of users per sector. A significant increase in capacity per cell is observed depending on the available channels to serve all the sectors. While a sector achieved a maximum capacity of 21 Mbps, three sectors achieved a total cell capacity of 63 Mbps. For a large availability of TVWS channels, the network would be further sectorized for even more capacity. It is worth noting that sectorisation is limited by the number of channels available and the system power, and usually, the maximum number of sectors per base station is six (6).

The impact of adopting the CPE separation to tackle interference and improve user capacity is evident compared to other studies which used separate channels for each remote CPE. In this study, for instance, three channels aggregation resulted to 5 Mbps capacity per user while serving 10 CPEs. In contrast, in the study by Masonta et al. (2015a, b), a similar range of coverage and base station EIRP resulted to around the same capacity per user for only 1 CPE which would have covered far fewer users. On the other hand, as the number of users grows—especially in sparsely populated areas—deploying a radio per remote becomes expensive and inefficient.

The relationship between the channel capacity and WSBS distance, R is shown in Figure 6 (a). As expected, there is a sharp rise in channel capacity when the target CPE is closer to the WSBS and a slow decay after surpassing a particular threshold distance value. This is caused by the deterioration in the received signal level, which fails to maintain the target SINR. Additionally, as R increases, D has to increase to maintain the required signal quality. However, as Equation (12) shows, there is an optimal value for D beyond which the channel capacity decreases as reflected in Figure 6 (a). As expected, Figure 6 (b) shows an N_S-fold increase in capacity by deploying N_S sectors in a cell.

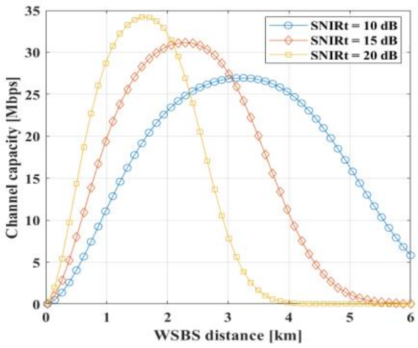

(a)

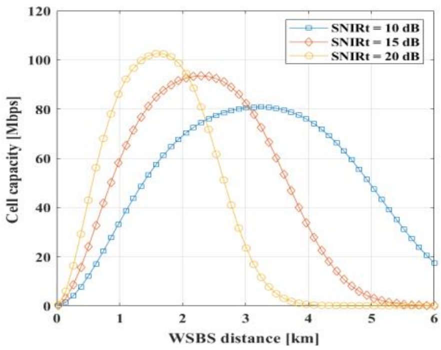

(b)

Figure 6: Capacity vs WSBS distance for N = 10.

In a sparsely populated setting, good coverage of a TVWS network would require the deployment of as many CPEs as possible to serve scattered users. Figure 7 shows the dependency of channel capacity to the number of CPEs in a network. It can be observed that the capacity increases with the number of CPEs (N) to the point of saturation, where further increase in N results in no increase in channel capacity. At the point of saturation, the increase in users will only result in the drop of the capacity per user as the channel is shared among the CPEs. Below the saturation point, the increment in capacity is visibly sharp, when the CPE distance (R) from the WSBS is smaller and becomes more slanted as R increases and the interference signal dominates. Usually, the increase in CPEs should result in rising of the interference and subsequent capacity drop; however, the CPEs distance distribution compensates for any possible SINR offset which maintains the channel capacity.

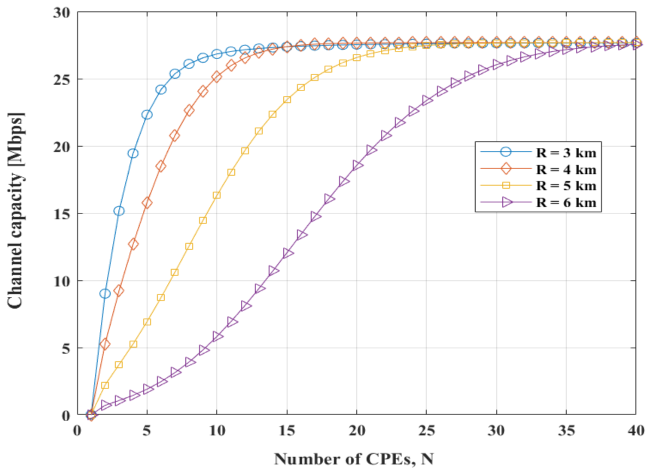

Figure 7: Variation of channel capacity with Number of CPEs for SINRt = 10 dB.

The impact of the base station's EIRP to the channel capacity is shown in Figure 8 (a). As shown in Equation (9), increasing P_w reduces D; however, for the given SINR, the rate of its decrease is less dominant below a threshold EIRP, resulting in the capacity increase. Beyond this threshold EIRP, dominance is significant and causes the capacity to decrease. As expected, Figure 8 shows the capacity improvement as SINR increases. Figure 8 (b) shows the increasing relationship between channel capacity and TVWD EIRP until a point where further increase in power degrades the capacity. Although from Equation (9), an increase in D is expected, which in turn should reduce interference; the rate of increase in TVWD EIRP coupled with the impact of D in the channel capacity causes the capacity to fall. Figure 8 (b) also shows that at small target SINR, high TVWD's EIRP can be accommodated as more interference is tolerated.

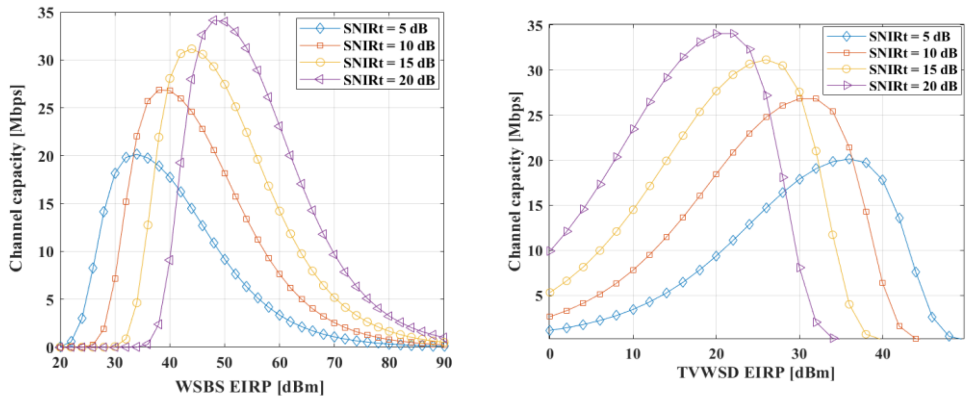

(a) (b)

Figure 8: Channel capacity vs EIRP for N = 10 and D_o = 3 km.

User capacity

One of the essential wireless network performance indicators is the capacity per user. Figure 9 shows how the capacity per user varies with CPEs separation and the CPE EIRP. Intuitively, there is a similar behaviour between the capacity per user in this case and the channel capacity in Figure 5 and Figure 8. However, while the trend is similar for different target SINR, it reverses when the number of nodes in the network is taken into account. Whereas the channel capacity increases with N in Figure 5 (a), the capacity per user decreases as shown in Figure 9 (a). This implies that the capacity per user is higher when there is a low number of users in the network. However, as expected, the low number of users ends up underutilizing the channel resulting in not fulfilling the expected channel capacity. Figure 9 (a) also shows the optimal separation between CPEs for a given target SINR (SINRt). It can be observed that, as N increases the optimal separation between CPEs—that can result in maximum user capacity—increases to compensate for the additional interference. As D depends on other parameters, as shown in (9), it is obtained in this case by varying one of the parameters while keeping the rest constant. Figure 9 (b) shows the relationship between the TVWD radiated power and the capacity per user for N = 10. The effect of the TVWD power on the user capacity is more severe when SINRt is high in which case the interference should be kept as low as possible. As SINRt decreases, it can be observed that more interferences are tolerated and the capacity decay is observed at a higher EIRP compared to the $SINR_t$ case.

In Figure 10, the impact of channel aggregation on user capacity is observed. The user capacity doubles if the channel bandwidth is doubled. For instance, for a $SINR_t$ of 10 dB, the capacity per user improves from 1.7 Mbps to 3.4 Mbps for a single level aggregation. Aggregating 3-channels results to a user capacity of approximately 5 Mbps at the same target SINR. Due to limited system power and availability of contiguous channels, channel aggregation is generally limited to 3 carriers. Aggregating inter-band or non-contiguous channels in the same band would result in further hardware complexities and costs. Again, the improvement in user capacity is visibly superior to the one obtained in the study by Masonta et al. (2015a, b) where a single channel per CPE was used to achieve an average capacity of around 4 Mbps.

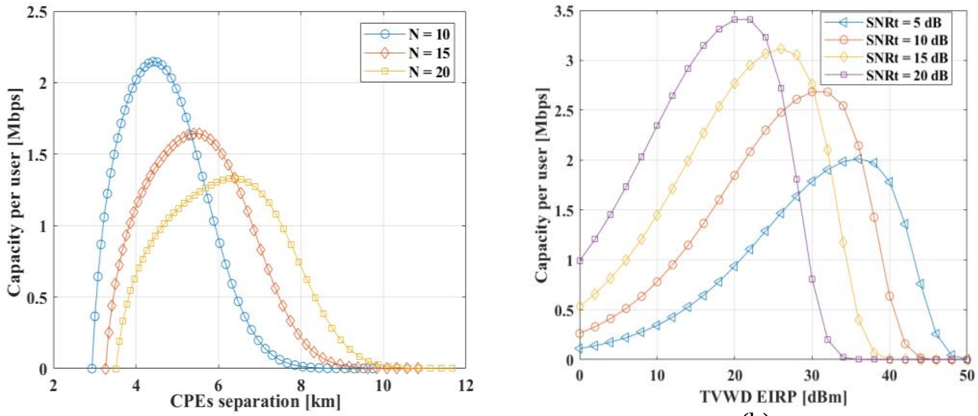

(a) (b)

Figure 9: Capacity per user for D_o = 5 km.

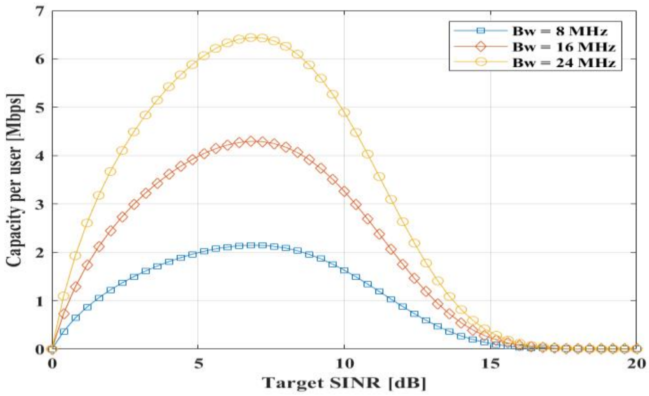

Figure 10: Capacity per user for different channel aggregation for D_o = 5 km.

Conclusion

This study aimed to analyze the radio network performance of the TVWS network deployed following a PPP CPE distribution in a channel environment characterized by the Hata propagation model. The study leveraged the distance between the CPE in sparsely populated areas (mostly rural areas) to achieve as high capacity as possible while covering as many potential users as possible. This paper has established the capacity analysis framework for TVWS network deployed based on the distance distribution approach–which is suitable for sparsely populated areas. It has been shown that with the distance distribution approach to CPEs deployment, it is possible to cover a large number of sparsely distributed users while optimizing the spectrum and power resources. The study considered equally spaced CPEs scenario and uniform devices configurations. However, in real-world deployment, the situation is likely to differ. The impact of CPEs spacing on the user capacity was evident, whereby at the target SINR of just 10 dB and WSBS range of 5 km the user capacity of approximately 2 Mbps was achieved. The actual TCP throughput is expected to be slightly higher due to less overheads in higher layers and error control. It is recommended that more studies–considering different CPEs configurations–on the TCP capacity and the impact of last-mile Wi-Fi extension on user throughput and CPE performance, be conducted.

References

Abu K and Ufoaroh SU 2019 Estimation and application of TV whitespaces for rural broadband connectivity (Internet Access). *Am. J. Eng. Res.* 8: 19–28.

Akinbolati A and Ajewole MO 2020 Investigation of path loss and modeling for digital terrestrial television over Nigeria. *Heliyon* 6(6): e04101.

Amine LM and Aawatif PH 2017 Toward enhancing connectivity through TVWS in outdoor rural isolated environment. *2017 Sensors Networks Smart and Emerging Technologies (SENSET)*, 1–4.

Dionisio R, Marques P and Rodriguez J 2015 Experimental assessment of a propagation model for TV white spaces. *Lecture Notes of the Institute for Computer Sciences, Social-Informatics and Telecommunications Engineering (LNICST)*, vol 146.

Dore JB, Ktenas D, Popon X, Dassonville D and Rosson P 2018 TVWS Field Trials with BF-OFDM. *2018 European Conference on Networks and Communications (EuCNC)*, Ljubljana, Slovenia, 2018, pp. 304-309.

Fanan AM, Riley N, Mehdawi M and Ammar M 2017 Comparison of propagation models with real measurement around Hull, UK. *24th Telecommunications Forum (TELFOR)*, Belgrade, 2016, pp. 1-4.

Gao R, Zhao Y, Wang Y and Yan T 2020 An improved propagation prediction model based on the okumura-hata model. *Adv. Intellig. Syst. Comp.* 905: 802-809.

Haenggi M 2005 On distances in uniformly random networks. *IEEE Trans. Info. Theory* 51(10): 3584–3586.

Hassan NU, Tushar W, Yuen C, Kerk SG, and Oh SW 2017 Guaranteeing QoS using unlicensed TV white spaces for smart grid applications. *IEEE Wireless Communications* 24 (2): 18–25.

Hessar F and Roy S 2015 Capacity considerations for secondary networks in TV white space. *IEEE Trans. Mobile Comput. 14* (9): 1780-1793.

IEEE 2011 IEEE Std 802.22 : Part 22: Cognitive Wireless RAN Medium Access Control (MAC) and Physical Layer (PHY) Specifications: Policies and Procedures for Operation in the TV Bands. *IEEE Comput. Soc*.

IEEE 2012 802.22.2-2012-IEEE recommended practice for information technology-telecommunications and information exchange between systems wireless regional area networks (WRAN)-specific requirements-Part 22.2: Installation and deployment of IEEE 802.22 system. *IEEE Comput. Soc*.

Miniwatts MG 2020 World internet users statistics and 2019 world population stats. url: https://www. internetworldstats. com/stats. htm [accessed 2020-07-28].

Ismail M, Kissaka MM and Mafole P 2019 Television white space opportunities and challenges: what next for the developing countries? *IST-Africa Week Conference (IST-Africa*), Nairobi, Kenya, 2019.

Johnson D, Zlobinsky N, Lysko A, Lamola M, Hadzic S, Maliwatu R and Densmore M 2016 Head to head battle of TV white space and wifi for connecting developing regions *8th EAI International Conference on E-Infrastructure and E-Services for Developing Countries (Africomm)*, Ouagadougou, Burkina Faso186-195.

Kalliovaara J, Paavola J, Ekman R, Kivinen A and Talmola P 2018 TV White Space Network Trials. In *TV White Space Communications and Networks* (pp. 121–149), Woodhead Publishing.

Karthipan R, Vishvaksenan KS, Kalidoss R and Suresh BR 2016 Uplink capacity enhancement in IEEE 802.22 using modified duplex approach. *Wireless Pers. Commun.* 86(2): 635–656.

Kumar A, Karandikar A, Naik G, Khaturia M, Saha S, Arora M and Singh J 2016 Toward enabling broadband for a billion plus population with TV white spaces. *IEEE Commun. Mag.* 54(7) : 28–34.

Lysko AA, Masonta MT, Mofolo MRO, Mfupe, Montsi, L, Johnson DL, Mekuria F, Ngwenya DW, Ntlatlapa NS, Hart A, Harding C and Lee A 2014 First large TV white spaces trial in South Africa: A brief overview. 6th *International Congress on Ultra Modern Telecommunications and Control Systems and Workshops (ICUMT)*, St. Petersburg, 2014, 407-414.

Masonta MT, Kola LM, Lysko AA, Pieterse L and Velempini M 2015a Network performance analysis of the Limpopo TV white space (TVWS) trial network. *AFRICON 2015*, Addis Ababa, 2015, 1-5.

Masonta MT, Ramoroka TM and Lysko AA 2015b Using TV white spaces and e-Learning in South African rural schools. *2015 IST-Africa Conference*, Lilongwe, 2015, 1-12.

Matogoro J, Mvungi NH and Justinian A 2018 Towards affordable broadband communication : a quantitative assessment of TV white space in Tanzania. In: Mekuria F, Nigussie E, Dargie W, Edward M and Tegegne T (Eds) *Information and Communication Technology for Development for Africa. ICT4DA 2017. Lecture Notes of the Institute for Computer Sciences, Social Informatics and Telecommunications Engineering*, vol 244 (pp 320-330), Springer, Cham.

Nyasulu T, Crawford D and Mikeka C 2018 Malawi's TV white space regulations : A review and comparison with FCC and Ofcom regulations. *2018 IEEE Wireless Communications and Networking Conference (WCNC),* Barcelona, 2018, 1-6.

Oh SW, Ma Y, Tao M, Chu E and Peh Y 2014 An overview and comparison of TV white space regulations worldwide. *International Conference on Frontiers of Communications, Networks and Applications (ICFCNA-2014 Malaysia),* Kuala Lumpur, 2014, 1-6.

Pazi S M and Chatwin CR 2013 Assessing the economic benefits and challenges of Tanzania's national ICT broadband backbone (NICTBB). *Int. J. Info. Comput. Sci.* 2(7): 117–126.

Stirling A and Beveridge J 2019 TVWS: From trial to commercial operation in the UK. In: Handbook of Cognitive Radio vol. 3 (pp 1919–1933).

Struzak R, Tjelta T and Borrego JP 2015 On radio-frequency spectrum management. *URSI Radio Sci. Bull.* 354: 11–35.

Sum C, Villardi GP, Rahman MA, Baykas T and Tran HN, Lan Z, Sun C, Alemseged Y, Wang J, Song C and Pyo CW 2013 Cognitive communication in TV white spaces: An overview of regulations, standards, and technology. *IEEE Commun. Mag.* 51(7): 138–145.

World Bank 2018 Innovative business models for expanding fiber-optic networks and closing the access gaps. http://documents.worldbank.org/curated/en/674601544534500678/pdf/132845-7-12-2018-17-20-11-InnovativeBusinessModels.pdf (accessed on 25/06/2020).

Yu SM and Kim S 2013 Downlink capacity and base station density in cellular networks. *2013 11th International Symposium and Workshops on Modeling and Optimization in Mobile, Ad Hoc and Wireless Networks (WiOpt),* Tsukuba Science City, 2013, 119–124.